Theoretical Studies on Competitive Binding of Caldesmon and Myosin S1 to Actin: Prediction of Apparent Cooperativity in Equilibrium and Slow-Down in Kinetics of S1 Binding by Caldesmon†

Bo Yan,[#] Anindita Sen,[‡] J. M. Chalovich,[‡,§] and Yi-der Chen[#,*]

Mathematical Research Branch, National Institute of Diabetes and Digestive and Kidney Diseases, NIH, Bethesda, Maryland 20892-5621, and Department of Biochemistry, East Carolina University Medical School, Greenville, North Carolina 27858-4354

Received December 4, 2002; Revised Manuscript Received February 10, 2003

ABSTRACT: Several laboratories have reported cooperative binding of S1 to actin in the presence of caldesmon. This cooperative binding has been interpreted with a model similar to that proposed for the binding of S1 to regulated actins in which the binding affinity of S1 is controlled by the position of the tropomyosin filaments. In a recent paper [Sen, A., Chen, Y., Yan, B., and Chalovich, J. M. (2001) *Biochemistry 40*, 5757−64], we showed qualitatively that S1 binding resulted in rapid dissociation of caldesmon from actin or actin-tropomyosin. This suggests that the cooperativity observed in the case of caldesmon is not due to a conformational change in actin-caldesmon but to the displacement of caldesmon. We show in this paper that the pure competitive binding model, in which both S1 and caldesmon are competing for the same binding sites on actin, can simulate quantitatively the effect of caldesmon on both the equilibrium and the kinetics of S1 binding to actin. This model successfully predicts an apparent cooperativity for the binding of S1 to actin-caldesmon without the need to assume multiple actin-caldesmon structures and produces a decreased rate of S1 binding to actin in the presence of caldesmon. This suggests that the inhibitory action of caldesmon on the actin-activated ATPase activity of myosin in solution and on the generation of active force in a contracting muscle may be simply due to the blocking of myosin binding sites on actin by caldesmon.

Caldesmon is an actin binding protein that inhibits actin-activated ATPase activity of myosin in solution (*2*) and force production in muscle fiber system (*3*−*5*). Inhibition of actin-activated ATP hydrolysis by caldesmon parallels the decrease in binding of S1-ATP[1] to actin (*6*−*9*). An important component of the inhibition of ATPase activity by caldesmon appears to be the inhibition of binding of myosin S1 to actin-tropomyosin (*6*, *10*). Image reconstructions of caldesmon-actin show that caldesmon overlaps the putative binding site of myosin-ATP on actin (*11*) in agreement with the competition of binding.

While there is agreement that caldesmon and myosin subfragments compete for binding in the absence of tropomyosin, some believe that in the presence of tropomyosin the competition of binding has only a minor role (*12*, *13*). They thus proposed that, like troponin-tropomyosin, caldesmon acts as an "allosteric" effector that controls the distribution between different actin states with different ATPase activities and S1 binding affinities.

Several factors contribute to this controversy and to the differences in interpretation of caldesmon function (*14*). One problem is in distinguishing binding of myosin to actin directly from interactions in which myosin is tethered by caldesmon. Caldesmon binds to myosin (*7*, *15*) as well as to actin (*2*), so a number of complexes are possible (*10*). The binding also depends on the ionic strength of the solution and the nucleotide bound to S1. As a result, large differences have been reported in the observed relationship between bound S1 and caldesmon bound to actin.

In a recent paper (*1*), we showed that this problem could be solved by placing different fluorescent probes on actin, S1, and caldesmon, respectively, so that each protein−protein interaction in the S1−actin−caldesmon complex can be monitored separately at equilibrium or as a function of time. We showed in the paper that: (i) Caldesmon reduced the rate of binding of rigor S1 to actin in the presence and absence of tropomyosin; (ii) No lag in the time course of binding of S1 to actin occurred in the presence of caldesmon and either in the presence or absence of tropomyosin; (iii) Binding of S1 to actin resulted in a rapid displacement of bound caldesmon. These results are qualitatively consistent with the notion that binding of caldesmon and S1 to actin is competitive. But a quantitative test of the model has not been carried out in that study.

† This work was supported by Grant AR35216 from the National Institutes of Health (to J.M.C.) and a predoctoral fellowship from the American Heart Association, North Carolina Affiliate (to A.S.).

* Correspondence to Yi-der Chen, NIDDK/NIH, 12 South DR RM 4007, MSC 5621, Bethesda, MD 20892-5621, Tel: 301-496-5436, Fax: 30-402-0535, E-mail: ydchen@helix.nih.gov.

[#] NIH.

[‡] East Carolina University Medical School.

§ Supported by Grant AR35216 from the National Institutes of Health.

[1] Abbreviations: EGTA, ethylene glycol-bis(β-aminoethyl ether)-*N*,*N*,*N*′,*N*′-tetraacetic acid; IANBD, *N*-((2-iodoacetoxy)ethyl)-*N*-methyl)-amino-7-nitrobenz-2-oxa-1,3-diazole; S1, myosin subfragment 1.

10.1021/bi0273009 CCC: $25.00
Published on Web 03/19/2003

In principle, there are at least two possible competitive models for binding two ligands to a double-stranded actin filament: the pure competitive and the mosaic models (*16*, *17*). In the former model, the two ligands compete for the same binding sites on actin so that each actin monomer can bind only one ligand, while in the latter model each ligand has its own binding site (e.g., one in the groove and one on the surface of the filament) so that both ligands can bind to the same actin monomer simultaneously. Recently, we have shown that the mosaic model works better for the equilibrium binding of AMPPNP−S1 and caldesmon to actin (*16*). In this paper, kinetic S1-chase measurements of the type described in Sen et al. (*1*) are analyzed quantitatively using a Monte Carlo simulation method to test whether the binding of rigor S1 and caldesmon to actin is pure competitive or mosaic. We first obtained the individual kinetic rate constants of binding S1 or caldesmon to actin using equilibrium and kinetic binding data measured separately for S1 or caldesmon alone. Kinetic curves of S1 binding to actin in S1-chase were then calculated theoretically using these kinetic rate constants and compared with those measured experimentally. We show that the measured kinetics of S1 binding in the S1-chase experiment can be simulated successfully with the *pure* competitive model, but not the mosaic model.

The effect of caldesmon on the equilibrium binding of S1 to actin was also studied theoretically for the pure competitive model using the same set of rate parameters obtained in this paper. It has been observed that the binding isotherm of S1 to actin in the presence of caldesmon is sigmoidal: the binding affinity is low at low S1 concentrations and high at high concentrations (*18*). This cooperative binding has been used to argue for the existence of multiple states for the actin filaments even in the absence of tropomyosin (*19*). We show in this paper that the apparent cooperative binding of S1 to actin in the presence or absence of tropomyosin can be simulated successfully with the pure competitive model. The results obtained in this paper strongly suggest that caldesmon inhibits S1 binding by directly competing for the same binding sites on actin.

The simulations shown here are generally applicable to other systems of binding of two or more ligands to a lattice of sites. An apparent cooperativity can occur when two of the ligands share common binding sites. In such cases, it is impossible to determine that there is a true allosteric effect without measuring the binding of both ligands to the lattice.

MODEL AND KINETIC SIMULATION

Two-Step S1 Binding Mechanism. Since the kinetic curves of binding S1 to actin in the absence of caldesmon can be interpreted by a double-exponential equation (*1*), we consider a two-step mechanism for binding of S1 to actin as suggested by Geeves (*20*). As shown in Figure 1A, step 1 results in the formation of a relatively weakly bound actin−S1 complex (the A-state) and state 2 represents the strongly bound state (the R-state) after isomerization of the complex. This mechanism is assumed to work both in the presence and absence of tropomyosin.

Pure and Mosaic Competitive Models. For simplicity, we assume that the number of actin monomers covered by a bound ligand is exactly seven for caldesmon and one for S1. In the pure competitive model (Figure 1B), both S1 and caldesmon are exclusively competing for the same binding site on each actin monomer. Thus, S1 cannot bind to an actin monomer, if the monomer is already bound with a caldesmon molecule, and vice versa. In the mosaic multiple-binding model (Figure 1C), in addition to open actin sites, S1 can also bind to some or all of the sites that are covered by a caldesmon with diminished affinities (see ref *16*). The pure competitive model can be obtained from the mosaic model by setting all the affinities of binding S1 to caldesmon-covered sites to zero. Cooperativity is assumed to exist between two neighboring caldesmon molecules (denoted as y_{22}) and between S1 and caldesmon (y_{12}).

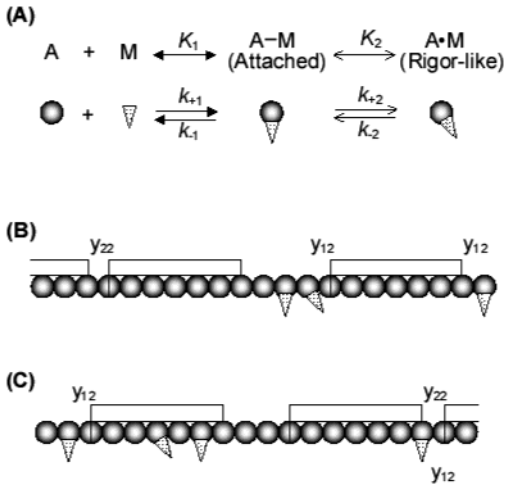

FIGURE 1: The pure competitive and mosaic multiple-binding models. (A) The two-step mechanism for the binding of S1 to actin: S1 binds to form the A-state first (binding at 90° to filament axis with equilibrium constant K_1), and then isomerizes to the R-state (binding at 45° with equilibrium constant K_2). (B) The pure competitive model (PC) of binding of S1 and caldesmon to actin where both S1 and caldesmon molecules are competing for the same binding site on each actin monomer. A bound caldesmon molecule (the rectangular box) can cover seven actin monomers while an S1 can cover only one actin monomer. (C) The mosaic multiple-binding model (MMB) in which S1 can bind to any of the seven actin monomers that are covered by a caldesmon molecule, except the one covered by the "head" part of the caldesmon. y_{12} is the cooperativity factor between S1 and caldesmon when bound next to each other on actin and is defined as $\exp(-w_{12}/k_BT)$, where w_{12} is the interaction energy, k_B is the Boltzmann constant, and T is the temperature. y_{22} is the cooperativity factor between two caldesmon molecules.

The binding of S1 and caldesmon to actin is schematically drawn in Figure 2 where each caldesmon is assumed to cover only four actin subunits for purposes of illustration. K_1 and K_2 are the equilibrium binding constants of S1 to bare actin sites for the two steps and K_1' and K_2' are those to sites covered by a caldesmon. Then, the quantities

$$\delta_1 = K_1'/K_1 \text{ and } \delta_2 = K_2'/K_2 \qquad (1)$$

can be used to characterize the degree of "deviation" from the pure competitive model. That is, the binding is pure competitive if δ_1 and δ_2 are equal to zero and of the mosaic type if they are not zero. The larger the δ, the farther away the binding is from the pure competitive model.

Let L_{ij} denote the binding constant of a caldesmon to a seven-actin-monomer unit bound with s $(= i + j)$ molecules of S1, in which i molecules are in the A state and j are in R state. Then $L_{ij} = L_{00}\delta_1^s\,\delta_2^j$. For simplicity, we assume $\delta_2 =$

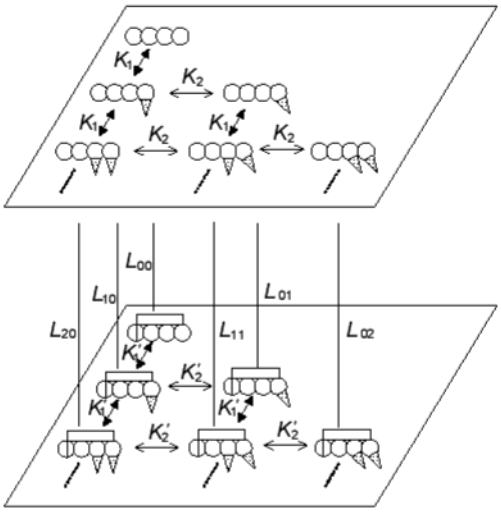

FIGURE 2: Diagram of the kinetics of binding of S1 and caldesmon to actin for the illustrative hypothetical case that each caldesmon molecule covers only four actin-sites. There are two layers that respectively represent the two-step mechanism of S1 binding to bare (upper layer) and caldesmon-bound (lower layer) actin. The reactions between the two layers represent the kinetics of caldesmon binding. L_{ij} is the binding constant of caldesmon to an actin unit with s ($= i + j$) molecules of bound S1, in which i molecules are in the A-state and j are in the R-state. In the PC model, only the reactions in the first layer and the special one between two layers ($s = 0$) are permitted while the rest are prohibited.

1, that is, bound caldesmon does not affect the isomerization of S1. Then the simplified relationships are

$$K_1' = K_1\delta,\ K_2' = K_2 \text{ and } L_s = L_0\delta^s \tag{2}$$

where $\delta \equiv \delta_1$ and $L_0 \equiv L_{00}$. Both K_i ($i = 1, 2$) and L_0 can be determined from equilibrium binding measurements, but not K_i' nor L_s. Thus, we treat δ as a parameter in our simulation.

Basic Rate Constants. The forward and backward rate constants of binding S1 (k_{+i} and k_{-i}, $i = 1, 2$) and caldesmon (l_+ and l_-) to actin can be evaluated independently and are used in the simulation without change. For the pure competitive model, these are the only rate constants that are needed in the simulation. For the mosaic multiple-binding model, additional information on the rate constants are required, because these rate constants depend on whether the actin monomers are bare or bound with ligands. Let k'_{+i} and k'_{-i} ($i = 1, 2$) represent the forward and backward rate constants of the two-step binding of S1 to a caldesmon covered actin monomer, and $l_+^{(s)}$ and $l_-^{(s)}$ denote those of a caldesmon binding to a 7-mer actin unit that has already bound with s molecules of S1, then they are related to those in the PC model as

$$k'_{+1}/k'_{-1} = K_1' = K_1\delta = (k_{+1}/k_{-1})\delta$$

$$k'_{+2}/k'_{-2} = K_2' = K_2 = k_{+2}/k_{-2} \tag{3}$$

$$l_+^{(s)}/l_-^{(s)} = L_s = L_0\delta^s = (l_+/l_-)\delta^s \tag{4}$$

where L_s is the equilibrium association constant between a caldesmon and a 7-mer actin unit that is bound with exactly s molecules of S1. The values of k_{+i} and k_{-i} ($i = 1, 2$), l_+ and l_- can be, respectively, determined by fitting the kinetics

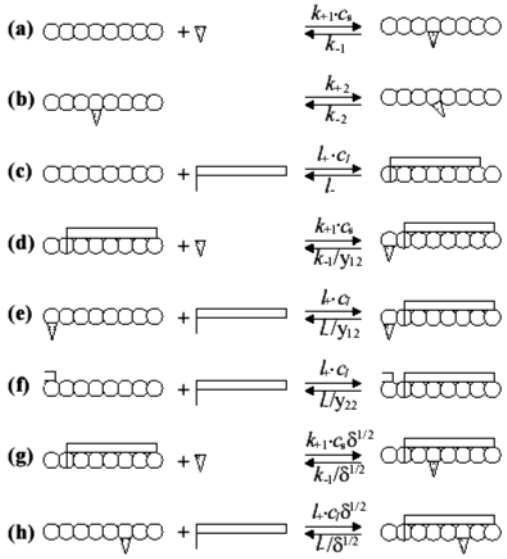

FIGURE 3: The rate constants of some basic reactions of the two models. Reactions (a, b) represent the two-step binding of S1 to a bare actin monomer and (c) represents the binding for caldesmon. c_s and c_l are the concentrations of free S1 and caldesmon in solution (they change with time and their calculations are given in the text). (d−f) are the reactions of binding of S1 or caldesmon to actin where its neighbor has already bound a caldesmon or S1 molecule. Cooperativity is assumed to exist only between S1 and caldesmon (y_{12}) and between two caldesmon molecules (y_{22}), and is assumed to affect only the dissociation rate. (g, f) represent the binding of S1 or caldesmon to a seven-actin monomer unit that is already occupied by a caldesmon or S1 in the MMB model. The parameter δ ($\equiv K_1'/K_1$) reflects the deviation of the binding from the PC model. Here the effect of δ is split evenly between the forward and backward steps.

of binding of S1 or caldesmon alone to actin using the Monte Carlo simulation method (*21*). Thus, with a given value of δ, eqs 3 and 4 can be used to estimate k'_{+i} and k'_{-i} ($i = 1, 2$) in terms of k_{+i} and k_{-i}, and $l_+^{(s)}$ and $l_-^{(s)}$ in terms of l_+ and l_-. However, there are many ways of assigning the individual rate constants that are consistent with eqs 3 and 4. For example, one can assign all of the effect of δ to the forward rate constant: $l_+^{(s)} = l_+\delta^s$, $l_-^{(s)} = l_-$. Or, one can put all of the effect to the backward rate constant: $l_+^{(s)} = l_+$, $l_-^{(s)} = l_-/\delta^s$. In this study, we separate the effect of δ evenly between the forward and the backward rate constants:

$$k'_{+1} = k_{+1}\delta^{1/2},\ k'_{-1} = k_{-1}/\delta^{1/2}$$

$$k'_{+2} = k_{+2},\ k'_{-2} = k_{-2} \tag{5}$$

$$l_+^{(s)} = l_+\delta^{s/2},\ l_-^{(s)} = l_-/\delta^{s/2} \tag{6}$$

Effect of Cooperativity. The cooperativity between two bound caldesmon molecules (y_{22}) is determined directly by fitting the equation of McGhee and von Hippel (*22*) to the equilibrium binding isotherm of caldesmon to actin (*21*). The cooperativity between S1 and the two ends of a caldesmon molecule (y_{12}) is assumed to be the same and treated as a parameter. For simplicity, cooperativity is assumed to affect only the dissociation rate constant, not the binding rate constant, as shown in Figure 3.

Monte Carlo Simulation of the S1 Chase. To evaluate the kinetics of binding of S1 and the dissociation of caldesmon in the S1 chase, we follow the transitions of a "single" actin

filament among its various "states" on a computer as a function of time and obtain the ensemble-averaged kinetic curve by repeating the process for a large number of times (*21*, *23*, *24*). That is, we treat the actual system as an ensemble of identical and independent "small" systems, each containing only one actin filament with ligands (S1 and caldesmon) in a small volume. The kinetics of the actual system is then represented by the ensemble average of the kinetics of a single small system. The state of an actin filament is specified by the number of bound S1 and caldesmon molecules and by the distribution of these molecules on the actin filament. The transition between any two (actin) states always involves binding or dissociation of either an S1 or a caldesmon molecule, or the isomerization of S1. The transition probabilities are therefore completely determined by the binding and the dissociation rate constants, the cooperativity factors, and the concentrations of free S1 and caldesmon molecules in solution. During the simulation, the concentrations of free S1 and caldesmon in solution change as a function of time, which can be evaluated using the following equations: $c_s = c_s^0 - (n_s/M)c_A^0$ and $c_l = c_l^0 - (n_l/M)c_A^0$, where c_s^0, c_l^0, and c_A^0 are the total concentrations of S1, caldesmon, and actin monomers respectively, n_s and n_l are the time-dependent numbers of bound S1 and caldesmon on an actin filament, and M is the total number of actin monomers in an actin filament ($M = 700$ in all calculations).

The program to simulate the S1 chase consists of two parts. At first, the equilibrium state of an actin filament is obtained by simulating the binding of caldesmon alone to a single actin filament in the absence of S1 until the number of bound caldesmon molecules becomes steady. Then, S1 is added to the system and the simulation resumes. Histograms showing the amount (number) of bound S1 and caldesmon as a function of time are obtained after S1 addition. The process is repeated a thousand times and the kinetic curves of S1 binding and caldesmon dissociation are obtained from the average of these histograms. The same Monte Carlo method can be used to simulate the caldesmon-chase experiment, in which the actin is preequilibrated with S1 first and then chase with caldesmon.

MATERIALS AND EXPERIMENTS

Skeletal actin (*25*, *26*) and myosin (*27*) were isolated from rabbit back and leg muscles. S1 was made by digesting myosin with chymotrypsin (*28*). Caldesmon was purified from turkey gizzards (*8*). Individual protein−protein interactions were monitored by the use of several fluorescent probes. In some cases, actin was labeled with *N*-(1-pyrene)iodoacetamide (*29*), myosin S1 was labeled with 5-iodoacetamidofluorescein on Cys 707 (*1*, *30*) and caldesmon was labeled with IANBD (*1*). The concentration of caldesmon was determined by the Lowry assay while the concentrations of other proteins were determined by absorbance at 280 and 340 nm (or 280 and 600 nm in the case of labeled proteins). The molecular weights used for calculation of protein concentration determination were (in Daltons) S1 (120 000), actin (42 000), tropomyosin (68 000), and caldesmon (87 000). The purity of all proteins was verified by polyacrylamide gel electrophoresis in the presence of SDS. A more detailed description of the protein preparations is given elsewhere (*1*).

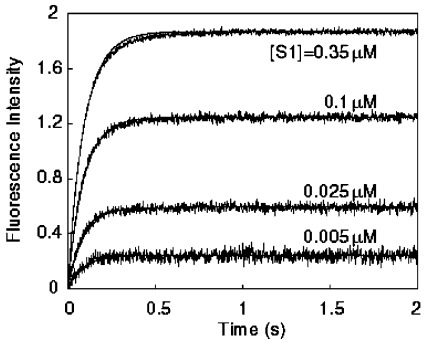

FIGURE 4: Time course of binding of fluorescein-labeled S1 to pure actin in the absence of caldesmon. The final concentration of actin was 3.5 μM. The concentrations of S1 were 0.35, 0.1, 0.025, and 0.005 μM. Each trace represents a computed average of three or four successive measurements. The solid lines are Monte Carlo simulations of the data using the parameters in Table 1.

Data Collection. All measurements were made at 15 °C in a buffer composed of 10 mM imidazole, 2 mM $MgCl_2$, 1 mM EGTA, 34 mM potassium propionate, and 1 mM dithiothreitol. Some of the parameters describing the binding of caldesmon to actin are from our earlier data (*8*, *21*). Additional equilibrium binding parameters for caldesmon and fluorescein S1 were taken from unpublished data.

Kinetic measurements were made on a DX17.MV/2 Sequential Stopped Flow spectrophotometer from Applied Photophysics. The excitation wavelength was controlled by a monochromator and a glass filter determined the emission wavelength. The kinetics of fluorescein-labeled S1 by rapidly mixing fluorescein S1 with actin and recording the time course of the fluorescence change. The mean rate constants were obtained by averaging over 20 sets of experiments with varied S1 and actin concentrations. Details about the experimental measurements can be found in an earlier paper (*1*).

The kinetics of competitive binding were measured by chase experiments in which an equilibrium mixture of actin and the first ligand was rapidly mixed with the second ligand. In most cases, the second ligand (chase ligand) had an attached fluorescent probe that reported the binding interaction. In S1 chase experiments, 7 μM actin with a variable amount of caldesmon were incubated at 15 °C for at least 10 min before mixing rapidly with an equal volume of 0.7 μM S1 in the stopped flow apparatus. A typical fluorescence intensity as a function of time after the S1 addition is similar to that shown in Figure 4, where the kinetic curves were obtained in the absence of caldesmon. A number of kinetic curves were obtained for caldesmon concentrations ranging from 0.1 to 1.0 μM (the final concentration). The time to one-half of the plateau (the half-time, $t_{1/2}$) of each fluorescence kinetic curve was evaluated either visually from the curve or analytically from the fitted equation and is plotted as a function of the caldesmon concentration in Figure 5A (in the absence of tropomyosin; open circles) and in Figure 5B (in the presence of tropomyosin; filled circles).

In the caldesmon chase experiment, 1 μM actin (with or without tropomyosin) was first equilibrated with S1 at different concentrations ranging from 0 to 1 μM. This solution was rapidly mixed with an equal volume of 0.1 μM NBD-caldesmon. The half-time, $t_{1/2}$, of the fluorescence change was then evaluated either visually or analytically from

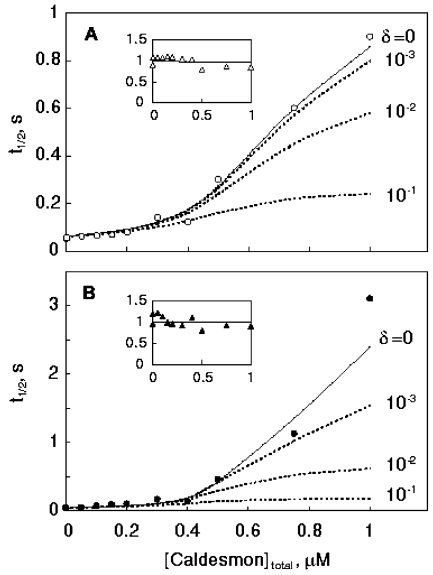

FIGURE 5: Dependence of the time for 50% completion of the binding of fluorescein-labeled S1 to actin with varied caldesmon concentrations in the absence (A) and presence (B) of smooth muscle tropomyosin. The simulated curves shown are for the pure competitive (the solid line, $\delta = 0$) and the mosaic (the dashed lines, $\delta \neq 0$) models with the parameters in Table 1. The insets show the normalized total fluorescence amplitudes and those simulated by the competitive model (solid lines). The protein concentrations after mixing were 3.5 μM actin-tropomyosin and 0.35 μM fluorescein-S1.

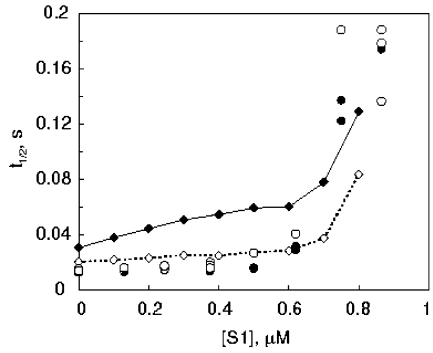

FIGURE 6: Dependence of the time for 50% completion of the binding of NBD-caldesmon to actin with varied S1 concentrations in the absence (white symbols) and presence (black symbols) of smooth muscle tropomyosin. The simulated curves were calculated in the two cases for the pure competitive model with the parameters in Table 1. Protein concentrations after mixing were 1.0 μM actin or actin-tropomyosin and 0.1 μM caldesmon.

an exponential fit to the data over the first 0.2 s of the kinetic curve. The results values of the half-time are shown as a function of the S1 concentration in Figure 6.

RESULTS

The Rate Constants and Cooperativity Parameters. The necessary parameters used in the calculations are listed in Table 1. All parameters except for the value of y_{12}, the cooperativity parameter between S1 and caldesmon, were obtained from equilibrium and kinetic binding measurements of S1 and caldesmon alone. The affinities of fluorescein-labeled S1 to actin obtained from binding isotherms were found to be 3.0×10^7 and 1.0×10^8 M^{-1} in the absence and presence of tropomyosin, respectively. These values are equal to $K_1(1 + K_2)$ in the two-step binding model. The

Table 1: Equilibrium Association Constants and Kinetic Rate Constants of Binding of Fluorescein-Labeled S1 and Caldesmon to Actin in the Presence and Absence of Tropomyosin

	without tropomyosin	with tropomyosin
	S1	
binding constants		
K_1/M^{-1}	1.5×10^5	5.0×10^5
K_2	200	200
rate constants		
$k_{+1}/M^{-1}\ S^{-1}$	3.7×10^6	4.6×10^6
k_{-1}/S^{-1}	24.7	9.2
k_{+2}/S^{-1}	160	160
k_{-2}/S^{-1}	0.8	0.8
	Caldesmon	
binding constants		
L_0/M^{-1}	5.5×10^5	2.0×10^6
y_{22}	20	21
rate constants		
$l_+/M^{-1}S^{-1}$	1.3×10^7	1.3×10^7
$l_-/^{-1}$	23.6	6.5
cooperativity		
y_{12}	1	1

equilibrium measurements do not contain sufficient information to define uniquely the two equilibrium constants. We assign K_2 a value of 200 based on the work of McKillop and Geeves ((*20, 31*) and see below). The kinetic rate constants of the two-step S1 binding, k_{+1}, k_{-1}, k_{+2}, and k_{-2} (only two are independent), were then determined by fitting a series of measured kinetic curves of S1 binding to actin at different concentrations of S1 using the Monte Carlo method described above as shown in Figure 4. We found that these fits were very sensitive to the value of k_{+1} but not to that of K_2 in the range between $K_2 = 20$ and 400 (data not shown). The values of k_{+1} in the absence and presence of tropomyosin were found to be 3.7×10^6 and 4.6×10^6 M^{-1} S^{-1}, respectively. These values are about 7 times larger than those obtained by Geeves and McKillop (*20*).

The equilibrium binding constant of caldesmon to actin (L_0) and the cooperativity between two bound caldesmon molecules (y_{22}) were obtained by fitting the binding isotherm of NBD-caldesmon to actin using the binding equation of McGhee and von Hippel (*22*). These fits gave L_0 in the absence and presence of tropomyosin of 0.55×10^6 and 2.0×10^6 M^{-1}, and y_{22} of 20 and 21, respectively. The kinetic rate constants, l_+ and l_-, were determined by fitting the measured kinetic curves of caldesmon binding to actin using the Monte Carlo method described in Chalovich et al. (*21*). The value of l_+ was found to be 1.3×10^7 M^{-1} S^{-1} both in the absence and presence of tropomyosin whereas that of l_- was found to be 23.6×10^6 and 6.5×10^6 S^{-1} respectively. That is, the enhanced binding of caldesmon to actin in the presence of tropomyosin is due primarily to a decrease in the rate constant of detachment as discussed before by Chalovich et al. (*21*).

All these parameters were used without change in modeling the S1-chase experiment. The only adjustable parameter is the cooperativity factor (y_{12}) between S1 and caldesmon. However, we found that the kinetics of S1 binding in the S1 chase changes very little when the value of y_{12} is varied between 1 and 1000. Thus, for simplicity, we have assigned the value of y_{12} to 1.

Fitting $t_{1/2}$ of S1 Binding Kinetics in the S1 Chase. The rate parameters given in Table 1 together with the measured

effect of caldesmon on the kinetics of S1 binding in the S1 chase were used to test whether the competitive binding of S1 and caldesmon to actin is of the pure-competitive (PC) or the mosaic-multiple binding (MM). There are several ways to analyze the effect of caldesmon on the kinetics of S1 binding. We can analyze directly each kinetic curve of fluorescence change caused by the binding of fluorescein-S1. This method is not practical, because there are too many kinetic curves to fit. It is also possible to fit each kinetic curve first with a two-exponential kinetic equation (see ref *1*) and then analyze the effect of caldesmon on the two "apparent" rate constants. In this paper, we measure the $t_{1/2}$, the time to reach 50% of the fluorescence change, from each kinetic curve and analyze that as a function of caldesmon. There are two reasons to use $t_{1/2}$, instead of the two "apparent" rate constants obtained in Sen et al. (*1*). First, the values of the two apparent rate constants obtained by fitting with a two-exponential equation are very sensitive to the time length of the kinetic curve used in the fitting. Thus, the two rate constants (especially the smaller one or the one controlling the long time behavior of the kinetics) cannot be accurately determined. Second, as described by Chalovich et al. (*21*), $t_{1/2}$ can be accurately measured and is useful for kinetic analyses.

Measured $t_{1/2}$ are shown as a function of the caldesmon concentration in the absence of tropomyosin in Figure 5A (open circles) and in Figure 5B (in the presence of tropomyosin). Also shown in Figure 5 are the theoretically calculated $t_{1/2}$ for the pure and mosaic competitive models based on the parameters listed in Table 1. Several interesting results can be seen from the figures. (i) Caldesmon decreases the rate of S1 binding; this decrease is particularly large in the presence of smooth muscle tropomyosin. The time for 50% completion of binding is increased by 16-fold (from 0.056 to 0.9 s) in the absence of tropomyosin and by 70-fold (from 0.042 to 3.0 s) in the presence of tropomyosin as the caldesmon concentration increases from 0 to 1.0 μM. (ii) As shown in the insets of the two figures, the final fluorescence amplitude did not change appreciably with increasing caldesmon concentrations. That is, while caldesmon drastically reduced the rate of S1 binding, caldesmon had little effect on the amount of S1 bound at equilibrium under these conditions. (iii) The half-time plots in Figure 5A,B were fitted quite well with the pure competitive model (PC), whereas the mosaic multiple-binding model ($\delta \neq 0$) always gave smaller $t_{1/2}$ values at the same caldesmon concentration (the fittings became better only when $\delta \leq 10^{-3}$). (iv) The amount of S1 bound at equilibrium was also reproduced well by the PC model at the same time (see the insets).

One must note that, in simulating the mosaic model, we have assigned the effect of δ evenly between the forward and the backward rate constants (see eqs 5 and 6). We have also carried out calculations for the extreme case that the effect of δ is only on the forward rate constant or only on the backward rate constant (data not shown). The same conclusions were reached although the simulated half-time curves were slightly different from those shown in Figure 5.

Fitting $t_{1/2}$ of Caldesmon Chase. We have also measured the kinetics of caldesmon binding in the caldesmon-chase experiments. Measured halftimes of the kinetic curves as a function of S1 concentrations are shown in Figure 6 along with those calculated for the pure competitive model using the parameters in Table 1. The level of agreement between the calculated and measured $t_{1/2}$ values in the presence and absence of tropomyosin is good. For actin-tropomyosin, the calculated halftimes deviated slightly from the experimental values. This indicates that the present model may be too simple for the competitive binding of S1 and caldesmon to actin-tropomyosin. Caldesmon does appear to cause a change in the position of tropomyosin on actin (*32*). Surprisingly, caldesmon stabilizes tropomyosin into a position that might be judged to be an activating state. While the significance of these two states is not understood, it is possible that smooth muscle actin-tropomyosin may exist in two or more states that differ in S1 binding. Currently, we are studying whether models that incorporate multiple states of tropomyosin-actin can explain the binding kinetics of both the S1-chase and the caldesmon-chase experiments. As in the S1-chase case, the mosaic model was also found unable to simulate the measured halftime curves at high S1 concentrations (data not shown).

Prediction of the Cooperative Binding of S1 to Actin-Caldesmon. The equilibrium binding of S1 to actin-tropomyosin in the presence of caldesmon has been shown to exhibit a cooperative type of behavior: S1 binding is low at low S1 concentrations and increases dramatically at high S1 concentrations. This result was used to argue for the notion that caldesmon might act as an allosteric effector similar to troponin-tropomyosin-actin in striated muscle. The idea is that actin-tropomyosin can exist in two states and caldesmon binding to actin stabilizes the low-affinity S1 binding state. With increasing concentrations of free S1, the high-affinity state would be favored leading to a cooperative increase in S1 binding. Recently, this model was suggested to work even when tropomyosin was absent (*19*). Here we show that the cooperative binding of S1 in the presence of caldesmon can be generated without invoking the two-state mechanism.

Figure 7 shows the binding isotherm of S1 to actin without tropomyosin calculated at different concentrations of caldesmon using the parameters listed in Table 1 for the pure competitive (panel A) and the mosaic (panel B) models. Panel A shows that the PC model can generate the cooperative binding of S1 to actin-caldesmon in the absence of tropomyosin, and the cooperativity is enhanced as the caldesmon concentration increases. Further simulations show that increasing the affinity of caldesmon ($L_0 \times y_{22}$) will enhance this cooperative binding whereas the affinity of S1 does not change the S-shape (data not shown). Panel B shows that the cooperative binding of S1 exists only when $\delta \leq 0.1$, and is inversely proportional to the value of δ. These findings suggest that the pure competitive binding model also works better in simulating the cooperative binding of S1 at equilibrium in the presence of caldesmon.

Lag in S1-ADP Binding to Actin. Another test for cooperativity in the actin filament is a delay or lag in the time course of binding of S1 (*20*, *24*). Pyrene labeled actin is often used to provide a measurable signal for binding and ADP is often included to increase the magnitude of the lag. Figure 8 shows the effect of caldesmon on the rate of binding of S1 to actin-tropomyosin under conditions in which a large lag was observed with troponin. In the absence of tropomyosin, the binding curve was adequately described by a

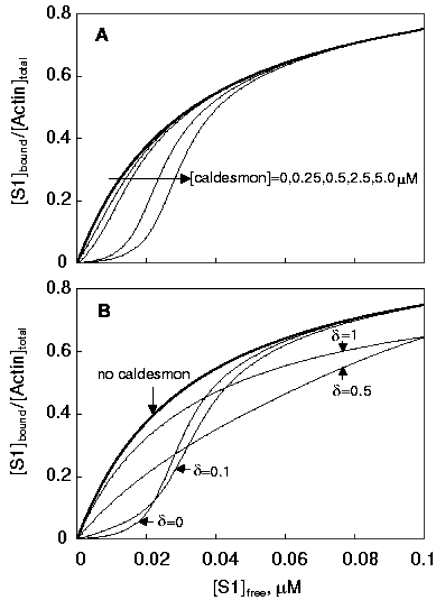

FIGURE 7: Cooperative binding of S1 to actin-caldesmon in the absence of tropomyosin predicted by the pure competitive (A) and mosaic (B) models. Panel A, the binding isotherms were calculated at different concentrations of caldesmon (from left to right: 0, 0.25, 0.5, 2.5, and 5.0 μM). Panel B, the binding isotherms were calculated at different δ (0, 0.1, 0.5, and 1.0) and 5.0 μM caldesmon. The thick line is the equilibrium binding of S1 in the absence of caldesmon. The concentration of actin was 3.5 μM.

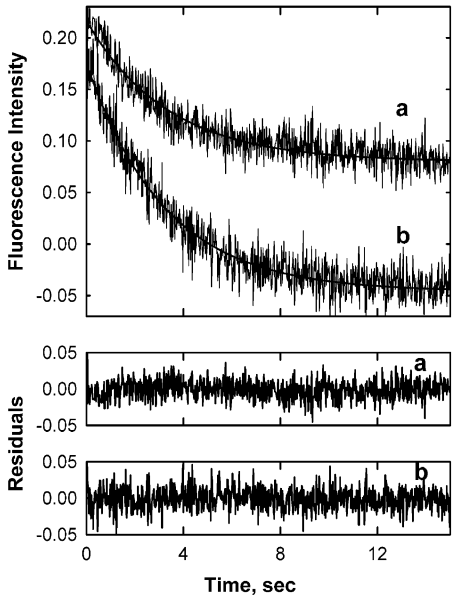

FIGURE 8: Time course of S1 binding to pyrene-labeled actin-tropomyosin. The final protein concentrations after mixing were: 2.5 μM S1, 0.5 μM actin, 0.11 μM tropomyosin, and either 1.12 (a) or 0.56 μM caldesmon (b). The solid curves are fits of monoexponential functions to the data. Residual plots (differences between the data and the exponential fits) for both curves are shown. A lag of 1−2 s was observed when troponin-tropomyosin was used in place of caldesmon-tropomyosin under identical conditions (not shown). Pyrene fluorescence was monitored with excitation at 344 nm with a 370 nm high pass filter. Conditions: 15 °C in buffer containing 2.5 mM MgADP, 1.9 mM $MgCl_2$, 200 mM NaCl, 33 mM potassium propionate, 20 mM imidazole (pH 7.0), 1 mM EGTA, and 1 mM dithiothreitol.

monoexponential function (not shown). Increasing concentrations of caldesmon were added to the actin-tropomyosin to increase the probability of stabilizing tropomyosin in a state that did not permit S1 binding. Caldesmon did reduce the rate of S1 binding (see Figure 5). However, Figure 8 shows that even high concentrations of caldesmon do not produce a lag in binding. The residual plots show that the exponential function provides an adequate description of the entire time course of the binding reaction. These results are another indication that inhibition of S1 binding by caldesmon is a direct effect that does not act through tropomyosin. As such, there are no long-range cooperative effects and no lag in binding.

DISCUSSION

Several observations suggest that caldesmon modulates smooth muscle contraction including: changes in caldesmon levels in the myometrium during pregnancy (*33*), the effects of caldesmon peptides on smooth muscle cells (*34*), and the effects of altering the concentration of caldesmon in smooth muscle cells (*35*) and in smooth muscle fiber bundles (*4*). Caldesmon inhibits the binding of myosin S1 to actin and actin-tropomyosin with an effectiveness that is related to the strength of the S1−actin interaction. Thus, caldesmon inhibits the equilibrium binding of S1-ATP (*6*) to a greater extent than that of S1-AMP−PNP (*7*, *16*) or rigor S1 binding (*1*). The preferential ability of caldesmon to inhibit attachment of actively cycling cross-bridges was also observed in skeletal muscle fiber studies (*3*). We suggest that the inhibition of binding of S1, particularly S1-ATP, to actin is a key factor in the inhibition of S1 ATPase activity by caldesmon (*1*, *6*, *10*).

Others have suggested that caldesmon functions more like the troponin-tropomyosin system by stabilizing an inactive conformation of actin-tropomyosin (*19*, *36*−*38*). To understand more clearly how caldesmon functions, it is necessary to better define the mechanism of binding of caldesmon and myosin to actin.

Several issues related to the regulation of smooth muscle contraction by caldesmon are addressed by the present analysis and by our recent kinetic data (*1*). First, the data and the present analysis show that caldesmon inhibits the binding of S1 to actin in the absence of nucleotide as well as in the presence of ATP. The affinity of caldesmon for actin is greater than that of S1-ATP for actin-tropomyosin and so caldesmon displaces S1-ATP from actin. In the rigor case, the affinity of S1 is greater than that of caldesmon so caldesmon does not readily displace S1. However, caldesmon does reduce the rate of binding of rigor S1 to actin. Therefore, the concept of competition holds true regardless of the nucleotide and both in the presence and absence of tropomyosin. As shown in Figure 5, tropomyosin actually enhances the ability of caldesmon to compete with S1 binding. This agrees with our earlier observation of equilibrium binding in the presence of AMP−PNP (*16*). Therefore it is not true that tropomyosin eliminates the ability of caldesmon to inhibit myosin binding. This is a basic difference between the behavior of caldesmon and troponin (*39*).

A second point involves the details of the competition between caldesmon and S1. Caldesmon is an elongated molecule and the common view is that caldesmon binds to several actin monomers. The exact number of monomers is controversial (*14*); this will be discussed in more detail in a future manuscript. Our view based on several kinds of

observation and outlined elsewhere (*16*) is that caldesmon binds most tightly to two or three actin monomers in an interaction involving the COOH-terminal region of caldesmon. The remainder of the caldesmon molecule does not bind as tightly and may not bind in the same way to actin. This raises the possibility that caldesmon may bind nonuniformly so that for a unit of about seven actin monomers, the attachment of S1 to some actin monomers may be inhibited to a greater extent than to others.

In the simplest case, caldesmon blocks the binding of S1 to all actin monomers covered by caldesmon. This is the pure competitive case. This model includes the possibility of interactions between adjacent caldesmon molecules and between caldesmon and S1 molecules. A more complex case is that of a mosaic of multiple binding sites in which S1 can still bind to some of the sites occupied by caldesmon. Our equilibrium binding data for the competition of S1-AMP−PNP and caldesmon were better simulated with the mosaic multiple binding model (*16*). However, the difference in predictions of the two models for the equilibrium case was small. We therefore turned to the kinetics of competition where our preliminary simulations suggested that the differences between the two models would be greater. Our present analysis indicates that the pure competitive model describes the S1 chase experiment very well both in the presence and absence of tropomyosin. The caldesmon chase experiment is well described by the pure competitive model in the absence of tropomyosin, but the model deviates from the data in the presence of tropomyosin. This indicates that in the presence of tropomyosin there are some factors that remain unaccounted for. However, the pure competitive model does describe the general features of binding in the presence of tropomyosin, and we will continue developing the model to explain the deviations where they occur.

The third point of this modeling relates to the proposal that caldesmon induces cooperativity into the actin or actin-tropomyosin filament that is similar to that observed with troponin. One group observed that caldesmon reduced the cooperative activation of the actin filament (*18*, *40*). Another group observed that caldesmon induced cooperative binding of S1 to actin even in the absence of tropomyosin (*19*). One might conclude that caldesmon is exerting these cooperative effects by stabilizing an inactive state of actin. This is the mechanism that has been proposed to occur in the case of troponin (*41*). However, there are significant differences between the troponin system and caldesmon that can affect the interpretation of these results. Of key importance, caldesmon and S1 compete with each other for binding to actin-tropomyosin (*1*, *6*, *10*), whereas troponin and S1 do not (*39*). In the case of caldesmon, the competition of binding could give the appearance of cooperativity. We have shown here that a pure competitive model can generate the cooperative binding of S1 in the presence of caldesmon without assumption of multiple actin states.

Our results provide an explanation for the observed cooperative binding of S1 to actin-caldesmon but do not exclude the possibility of caldesmon-induced cooperativity of actin. Nevertheless, until earlier results have been corrected for competitive interactions any conclusions that caldesmon induces cooperativity are tenuous. Any observations designed to show that caldesmon induces cooperativity in S1 binding must include an analysis of the amount of both caldesmon and S1 that are bound to actin.

The cooperative troponin-tropomyosin system is also characterized by a lag in the binding of S1 when S1 is in excess over actin (*20*, *24*). A lag in the binding of S1 to actin would have been expected if caldesmon functioned like troponin in stabilizing tropomyosin in an inactive state that could be reversed by S1 binding. We showed earlier that there is no such lag for binding of fluorescein-labeled S1 to actin-tropomyosin in the presence of caldesmon (*1*). A more common way to study a delay in S1 binding to actin is to monitor the binding of S1 to pyrene labeled actin. In the case of troponin, the lag is particularly large in the presence of ADP (*39*). As shown in Figure 8 no lag was seen for binding of S1-ADP to pyrene-labeled actin-tropomyosin even in the presence of a large excess of caldesmon. This is another instance in which the behavior of caldesmon-tropomyosin differs from that of troponin-tropomyosin.

In conclusion, we have developed a Monte Carlo strategy to simulate the kinetic and equilibrium binding of S1 to actin in the presence of caldesmon. This strategy is very useful in elucidating the mechanisms of the caldesmon−actin−S1 interaction. We have shown that a pure competitive model in which the two ligands are exclusively competing for the same binding sites on actin could successfully explain all known features in the kinetics and equilibrium measurements. This suggests that the inhibitory action of caldesmon on actin-activated ATPase activities of myosin in solution or the force generated in a contracting muscle fiber may be caused by a reduction of actin sites for myosin binding. This model will be extended to predict the inhibition of ATPase activity by caldesmon binding to actin in the presence or absence of tropomyosin.

ACKNOWLEDGMENT

The authors thank Michael Vy-Freedman for expert technical assistance and Swift-Eckrich Inc. for supplying turkey gizzards.

REFERENCES

1. Sen, A., Chen, Y., Yan, B., and Chalovich, J. M. (2001) *Biochemistry 40*, 5757−64.
2. Sobue, K., Muramoto, Y., Fujita, M., and Kakiuchi, S. (1981) *Proc. Natl. Acad. Sci. U.S.A. 78*, 5652−5.
3. Brenner, B., Yu, L. C., and Chalovich, J. M. (1991) *Proc. Natl. Acad. Sci. U.S.A. 88*, 5739−43.
4. Pfitzer, G., Zeugner, C., Troschka, M., and Chalovich, J. M. (1993) *Proc. Natl. Acad. Sci. U.S.A. 90*, 5904−8.
5. Malmquist, U., Arner, A., Makuch, R., and Dabrowska, R. (1996) *Pflugers Arch. 432*, 241−7.
6. Chalovich, J. M., Cornelius, P., and Benson, C. E. (1987) *J. Biol. Chem. 262*, 5711−6.
7. Hemric, M. E., and Chalovich, J. M. (1988) *J. Biol. Chem. 263*, 1878−85.
8. Velaz, L., Hemric, M. E., Benson, C. E., and Chalovich, J. M. (1989) *J. Biol. Chem. 264*, 9602−10.
9. Velaz, L., Ingraham, R. H., and Chalovich, J. M. (1990) *J. Biol. Chem. 265*, 2929−34.
10. Sen, A., and Chalovich, J. M. (1998) *Biochemistry 37*, 7526−31.
11. Lehman, W., Vibert, P., and Craig, R. (1997) *J. Mol. Biol. 274*, 310−7.
12. Marston, S. B., and Huber, P. A. (1996) in *Biochemistry of Smooth Muscle Contraction* (Barany, M., Ed.) pp 77−90, Academic Press, San Diego.
13. Redwood, C. S., and Marston, S. B. (1993) *J. Biol. Chem. 268*, 10969−76.

14. Chalovich, J. M., Sen, A., Resetar, A., Leinweber, B., Fredricksen, R. S., Lu, F., and Chen, Y. (1998) *Acta Physiol. Scand. 164*, 427−35.
15. Ikebe, M., and Reardon, S. (1988) *J. Biol. Chem. 263*, 3055−8.
16. Chen, Y., and Chalovich, J. M. (1992) *Biophys. J. 63*, 1063−70.
17. Chen, Y. (1990) *Biopolymers 30*, 1113-21.
18. Marston, S. B., Fraser, I. D., and Huber, P. A. (1994) *J. Biol. Chem. 269*, 32104−9.
19. Ansari, S., El-Mezgueldi, M., and Marston, S. B. (2002) *Biophys. J. 82*, 375A.
20. McKillop, D. F., and Geeves, M. A. (1991) *Biochem. J. 279*, 711−8.
21. Chalovich, J. M., Chen, Y., Dudek, R., and Luo, H. (1995) *J. Biol. Chem. 270*, 9911−6.
22. McGhee, J. D., and von Hippel, P. H. (1974) *J. Mol. Chem. 86*, 469−89.
23. Chen, Y., and Hill, T. L. (1983) *Proc. Natl. Acad. Sci. U.S.A. 80*, 7520−3.
24. Chen, Y., Yan, B., Chalovich, J. M., and Brenner, B. (2001) *Biophys. J. 80*, 2338−49.
25. Eisenberg, E., and Kielley, W. W. (1972) *Cold Spring Harbor Symp. Quant. Biol. 37*, 145−152.
26. Spudich, J. A., and Watt, S. (1971) *J. Biol. Chem. 246*, 4866−71.
27. Kielley, W. W., and Harrington, W. F. (1960) *Biochim. Biophys. Acta 41*, 401−421.
28. Weeds, A. G., and Taylor, R. S. (1975) *Nature 257*, 54−6.
29. Kouyama, T., and Mihashi, K. (1981) *Eur. J. Biochem. 114*, 33−8.
30. Lin, Y., Ishikawa, R., and Kohama, K. (1993) *J. Biochem. (Tokyo) 114*, 279−83.
31. McKillop, D. F., and Geeves, M. A. (1993) *Biophys. J. 65*, 693−701.
32. Hodgkinson, J. L., Marston, S. B., Craig, R., Vibert, P., and Lehman, W. (1997) *Biophys. J. 72*, 2398−404.
33. Word, R. A., Stull, J. T., Casey, M. L., and Kamm, K. E. (1993) *J. Clin. Invest. 92*, 29−37.
34. Katsuyama, H., Wang, C. L., and Morgan, K. G. (1992) *J. Biol. Chem. 267*, 14555−8.
35. Earley, J. J., Su, X., and Moreland, R. S. (1998) *Circ. Res. 83*, 661−7.
36. Borovikov, Y. S., Avrova, S. V., Vikhoreva, N. N., Vikhorev, P. G., Ermakov, V. S., Copeland, O., and Marston, S. B. (2001) *Int. J. Biochem. Cell Biol. 33*, 1151−9.
37. Marston, S. (1988) *FEBS Lett. 238*, 147−50.
38. Marston, S. B., and Redwood, C. S. (1993) *J. Biol. Chem. 268*, 12317−20.
39. Resetar, A. M., Stephens, J. M., and Chalovich, J. M. (2002) *Biophys. J. 83*, 1039−49.
40. Horiuchi, K. Y., and Chacko, S. (1989) *Biochemistry 28*, 9111−6.
41. Hill, T. L., Eisenberg, E., and Greene, L. (1980) *Proc. Natl. Acad. Sci. U.S.A. 77*, 3186−90.

BI0273009